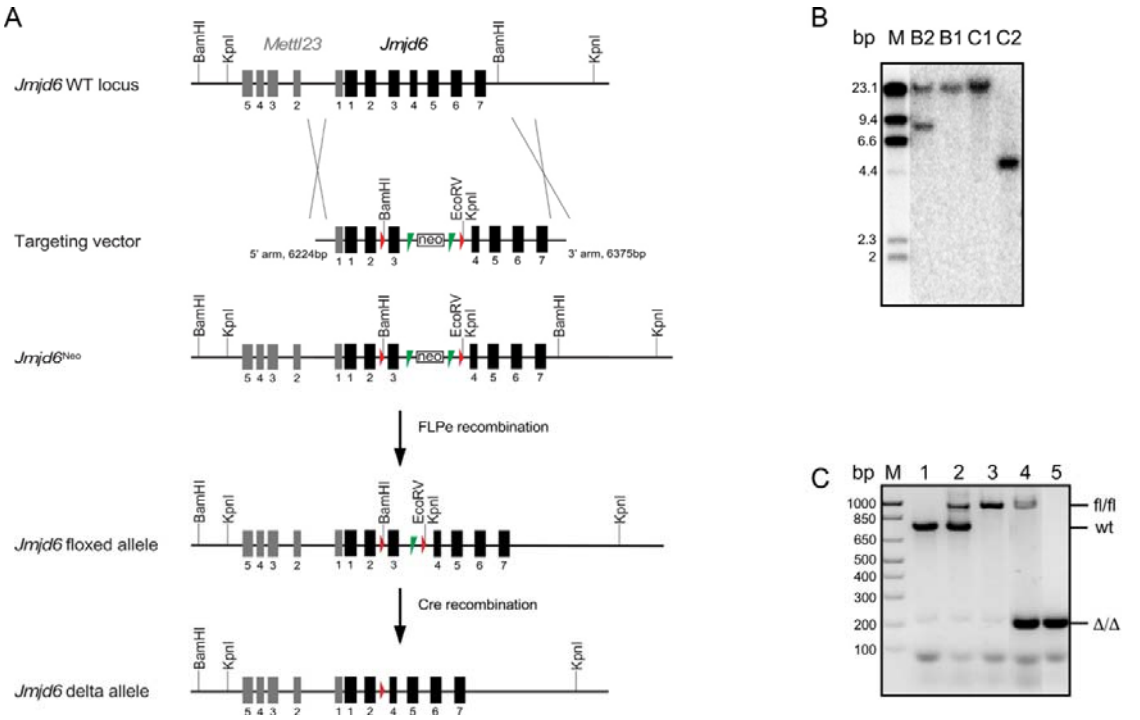

Figure S1. Generation of conditional *Jmjd6* knockout mice. (A) Targeting strategy for the generation of the *Jmjd6*$^{fl/fl}$ allele. The WT locus of JMJD6 is presented (top). The targeting vector including two loxP sites (illustrated by red rectangles) surrounding exon 3 are shown. FRT sites flanking the neomycin (neo) resistance cassette are illustrated by green triangles. The targeted (*Jmjd6Neo*), and *Jmjd6*$^{fl/fl}$ allele are also shown with the BamHI, EcoRV and KpnI restriction enzyme sites. At the bottom is the domain structure of the *Jmjd6* delta allele following Cre recombination. **(B)** Southern blot of *Eco*RV-digested genomic DNA from progenies of *Jmjd6*$^{+/flox}$ x *Flpe* breeding. Expected sizes: 31.4 kb for the WT allele, 8.3 kb for the *Jmjd6*^{fl} allele with deleted neomycin cassette. M, molecular weight marker (λ-DNA, HindIII digest); B2, heterozygote mouse with WT allele over flox allele after FLPE-mediated deletion of neomycin cassette; B1, WT; C1 and C2, control DNAs (C1 = C57BL/6J, C2 = probe containing plasmid). **(C)** Representative gel of a PCR reaction using genomic DNA extracted from murine ear notches. M, molecular weight marker (1kb); 1, PCR product from wt mice (approx. 750bp); 2, PCR products from heterozygous (+/flox) mice (wt = approx. 750bp, floxed = approx. 1kb); 3, PCR product from homozygous flox/flox (*Jmjd6*^{fl}) mice (approx. 1kb); 4, PCR products from flox/Δ mice, the progeny of *Jmjd6*^{fl} mice crossed with *Cre* transgenic mice (floxed = approx. 1kb, Δ approx. 200bp); 5, PCR product from *Jmjd6*^{fl} mice with *Cre*-mediated deletion i.e. *Jmjd6*^{cKO}mice (approx. 200bp).

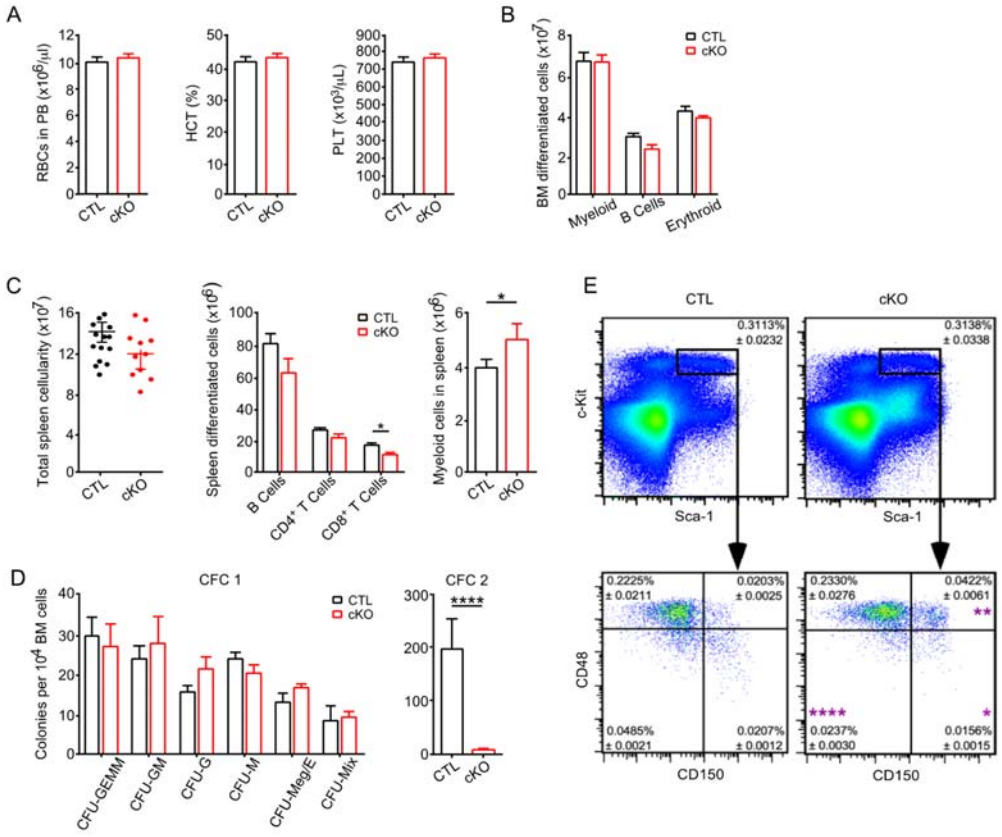

Figure S2. Hematopoietic-specific deletion of *Jmjd6* in young mice. (A) Peripheral blood (PB) analyses of *Jmjd6*^{cKO} and *Jmjd6*^{CTL} 8- to 10-week-old mice. Levels of red blood cells (RBCs), hematocrit (HCT) and platelets (PLT) (n=9-10). **(B)** Total numbers in BM of CD11b^{+}Gr1^{+} myeloid cells, CD19^{+}B220^{+} B cells and Ter119^{+} erythroid cells of 8- to 10-week-old *Jmjd6*^{cKO} and *Jmjd6*^{CTL} mice (n=13-16). **(C)** Total spleen cellularity, number of B cells, CD4^{+} T cells, CD8^{+} T cells and myeloid cells of *Jmjd6*^{cKO} and *Jmjd6*^{CTL} 8- to 10- week-old mice (n=11-14). **(D)** CFU assays performed with BM cells from 8- to 10-week-old *Jmjd6*^{cKO} and *Jmjd6*^{CTL} mice. Colonies were counted and scored 10 days after plating. CFC 1: CFU-GEMM, CFU-granulocyte, erythroid, macrophage or megakaryocyte; CFU-GM, CFU-granulocyte and monocyte/macrophage; CFU-G, CFU-granulocyte; CFU-M, CFU-monocyte/macrophage; CFU-Meg/E, CFU-megakaryocyte and erythroid burst-forming units; CFU-Mix, granulocyte, erythroid, macrophage and megakaryocyte (n=12-13). CFC 2: *Jmjd6*^{cKO} and *Jmjd6*^{CTL} cells from CFC-1 were re-plated 10 days after initial plating. Total numbers of colonies were counted after 10 days in culture (n=12-13). **(E)** Representative FACS profiles showing frequencies (± SEM) of BM LSKs, LSKCD48^{-}CD150^{+} HSCs, LSKCD48^{-}CD150^{-} MPPs, LSKCD48^{+}CD150^{-} HPC-1 and LSKCD48^{+}CD150^{+} HPC-2 populations from 8- to 10-week-old *Jmjd6*^{cKO} and *Jmjd6*^{CTL} mice (n=13-16). Data represent mean ± SEM; *p < 0.05; **p < 0.01; ****p < 0.0001 (Mann-Whitney U test).

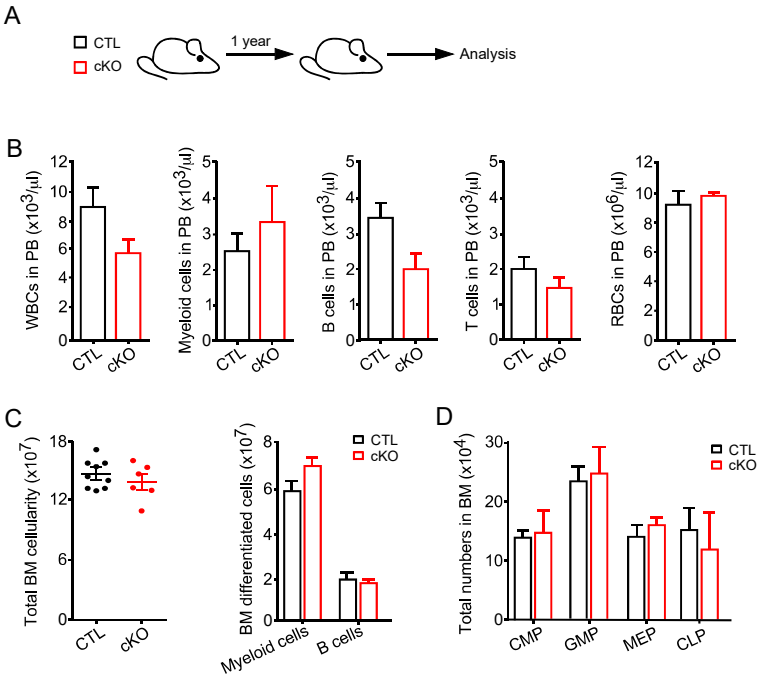

Figure S3. The impact on hematopoietic-specific deletion of *Jmjd6* on ageing. **(A)** Experimental design. *Jmjd6*^{cKO} and *Jmjd6*^{CTL} mice were aged for one year followed by analyses of their steady state hematopoiesis. **(B)** PB analyses of *Jmjd6*^{cKO} and *Jmjd6*^{CTL} 52-week-old mice. Counts of white blood cells (WBCs), myeloid cells, B cells, T cells and RBCs (n=6-9). **(C)** Total BM cellularity, number of myeloid cells and B cells of *Jmjd6*^{cKO} and *Jmjd6*^{CTL} 52-week-old mice (two femurs and two tibias) (n=6-9). **(D)** Total numbers in BM of common myeloid progenitors (CMP; LKCD34^{+}FcγRII/III^{low}), granulocyte-macrophage progenitors (GMP; LKCD34^{+}FcγRII/III^{high}), megakaryocyte-erythroid progenitors (MEP; LKCD34^{-} FcγRII/III^{low}), and common lymphoid progenitors (CLP; Lin^{-}Sca-1^{low}c-Kit^{low}CD127^{+}CD135^{+}) of 52-week-old *Jmjd6*^{cKO} and *Jmjd6*^{CTL} mice (n=5-8). Data represent mean ± SEM.

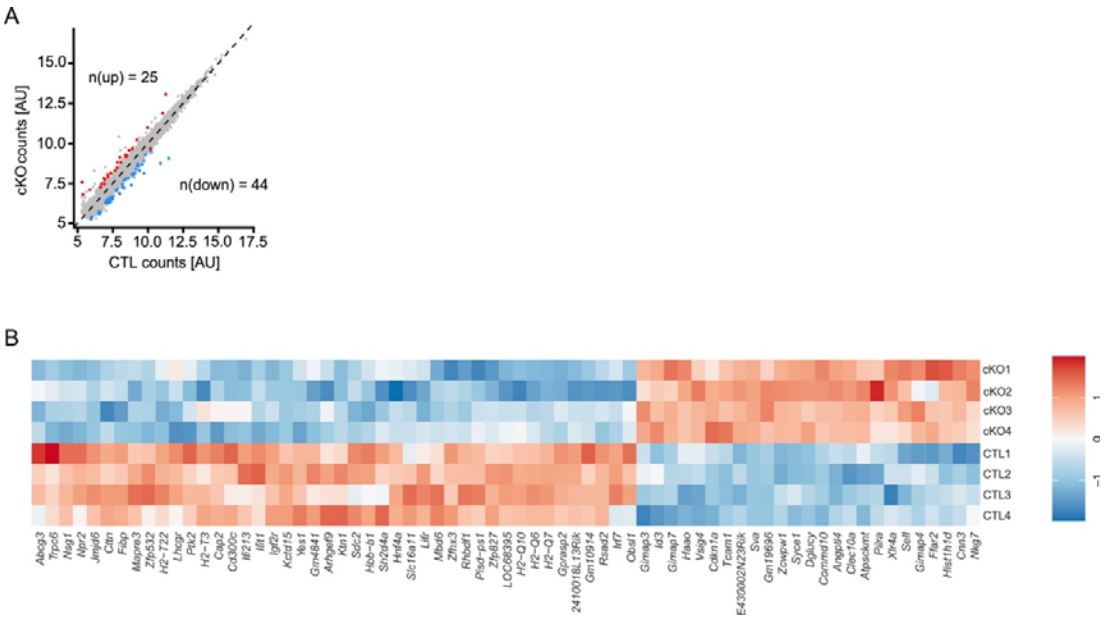

Figure S4. *Jmjd6*-deficient HSCs display a specific molecular signature impeding HSC maintenance and self-renewal. (A) Expression scatter-plot of *Jmjd6*^{cKO} samples vs controls. Significantly dysregulated transcripts up (red) and down-regulated (blue) in *Jmjd6*^{cKO} are highlighted (FDR < 0.05 and fold change > 20%) (n=4 per genotype). **(B)** Expression z-scores (based on log2-transformed FPKM values) for each sample for up and down-regulated genes indicated in Figure S4A.

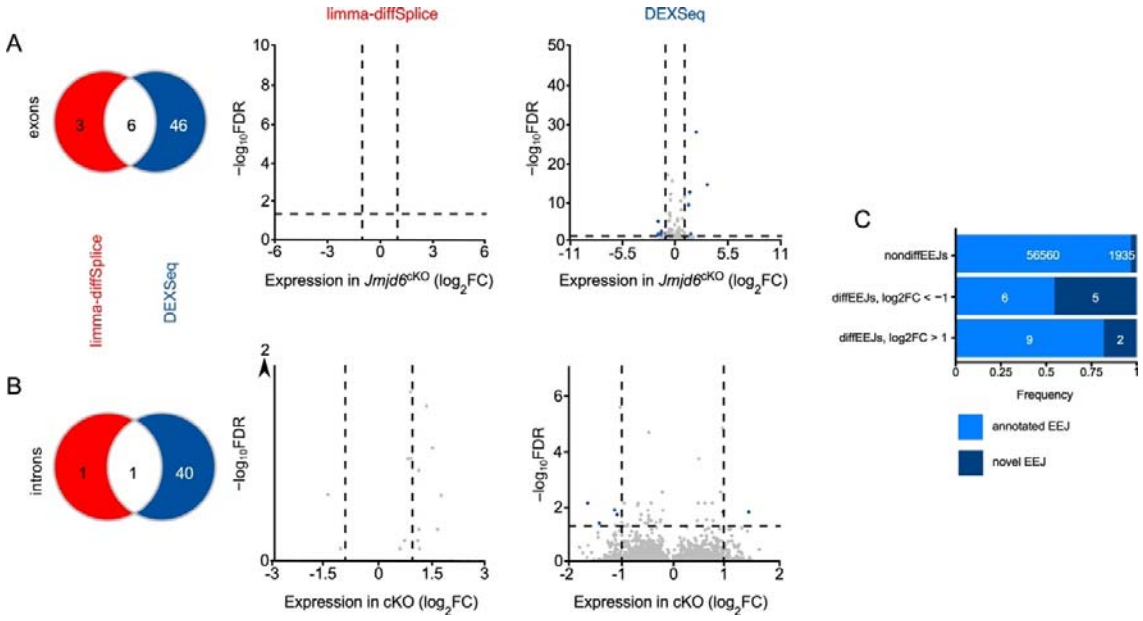

Figure S5. JMJD6 is not a major regulator of splicing in HSCs. (A, B) Assessment of expression in exons **(A)** and introns **(B)** by limma-diffSplice (red) and DEXSeq (blue). Left panels: Venn diagrams comparing differentially-expressed exons or introns identified by limma-diffSplice and DEXseq. Middle and right panels: volcano plots of differential expression in exons and introns identified by limma-diffSplice (middle) or DEXSeq (right). **(C)** Analysis of annotated (light blue) and novel (dark blue) exon-exon junctions identified from Gencode basic transcripts in Ensembl 91. Differential expression was assessed by QoRTs-JunctionSeq from RNA-seq reads overlapping splice donor and acceptor sites. EEJ dysregulation was identified where $|\log_2 FC| > 1$ and FDR < 0.05, event counts displayed in white.